19th International Conference on
Adaptive Structures and Technologies
October 6-9, 2008
Ascona, Switzerland

Thermomechanical Characterization of Shape Memory Polymers

Brent L. Volk[1], and Dimitris C. Lagoudas[1]
[1] Aerospace Engineering Department, Texas A&M University, College Station, TX 77843-3141
*lagoudas@tamu.edu, Phone: (979) 845-9409, Fax: (979) 845-6051

ABSTRACT

This study presents the testing methodology and equipment used for thermomechanical characterization of a shape memory polymer (SMP). The experiments performed include uniaxial tensile tests of 10, 25, 50, and 100% extension. The ability for a SMP to recover an applied deformation, known as the shape memory effect, requires a complex thermomechanical cycle and experimental setup. A visual-photographic apparatus was used to measure and record the distributed strain field in the gage section. Using this strain measurement system, the deformation is captured at multiple material points and compared for homogeneity. The results from representative tensile tests are presented, in which the complete shape memory effect is captured for dogbone specimens. Finally, the stress-strain and strain-time relationships are compared for different values of applied extension.

Keywords: Shape memory polymers, thermomechanical characterization, shape memory effect

1. INTRODUCTION

Shape memory polymers (SMPs) are polymers capable of recovering an applied strain through thermal, optical, and/or electrical actuation. SMPs represent a relatively new class of shape memory materials, which also includes shape memory alloys (SMAs) and shape memory ceramics. Shape memory materials have been widely researched, developed, and utilized in a wide range of applications, including cutting-edge technologies in the aerospace, medical, and oil exploration industries [1-3].

Although both SMPs and SMAs have the ability to recover an apparently permanent deformation, SMPs possess the unique ability to recover strains of up to 400% [4]. In addition, SMPs are lightweight, inexpensive, and possess excellent manufacturability characteristics compared to SMAs. On the other hand, SMPs typically have stiffness, strength, and actuation stress values two to three orders of magnitude lower than their metal counterparts [5-10]. Consequently, SMPs present a viable solution for applications, such as space and biomedical, which demand large deformations at reduced force levels. Other possible applications for shape memory polymers include biodegradable sutures, repairable automobile skins, satellites and deployable space systems [6,9,11]. Additional research efforts have focused on increasing the naturally low stiffness and low recovery stress of SMPs via the development of composites, which incorporate shape memory polymer as the matrix material [11-15].

Initial experimental efforts by Tobushi, et al. provided data from small deformation experiments [16], including experiments with applied extensions of 2%, 4%, and 10%. The tests

investigated the stress-strain relationship of thin film, polyurethane SMPs. Additional efforts by Tobushi, et al. included extending the thin films to 20% and 100% [8]. The thermomechanical response was captured for specimens which were loaded at different temperatures. The preliminary cyclic effects on the shape recovery were investigated. Further efforts were conducted by Liu, et al. on the thermomechanical behavior of SMPs for small extensions [5]. These experiments characterized dogbone shaped specimens, and provided evidence of the nonlinear strain recovery behavior with respect to temperature. The magnitude of the maximum applied extension was 9%, and the stress increase due to constrained cooling was captured. Additionally, Atli, et. al thermomechanically characterized SMPs for applied tensile extensions up to 75% [17]; however, the complete strain recovery profile during heating was not captured.

The objective of this work is to establish a more complete understanding of the basic thermomechanical aspects of shape memory polymers. As part of this work, the complete strain recovery profile will be captured for a wide range of deformations (10 to 100% extension) applied to specimens conforming to ASTM standards. In Section 2, the thermomechanical cycle necessary to extract the shape memory effect is outlined and connected with the state of the molecular chains during each thermomechanical segment. Section 3 presents the details of the experimental setup, the material preparation, and the thermomechanical loading parameters. Finally, Section 4 compares deformation results at multiple material points along the gage length, and provides results for thermomechanical experiments in which extensions of 10, 25, 50, and 100% are applied to the specimens.

2. SHAPE MEMORY EFFECT

The ability for shape memory polymers to recover a seemingly permanent deformation is known as the shape memory effect (SME). Although the shape memory effect can be triggered thermally, electrically, magnetically, or electromagnetically [6,9], this work will focus on the thermally activated SMPs. In general, the structure of a shape memory polymer can take a variety of forms. For instance, SMPs can take the form of chemically cross-linked glassy thermosets, chemically cross-linked semi-crystalline rubbers, physically cross-linked thermoplastics, or physically cross-linked block copolymers [9].

2-1. Thermomechanical Cycle

All four types of shape memory polymers can recover an applied deformation, and the molecular mechanisms which account for the shape recovery have been discussed in depth by Liu, et. al. as well as Lendlein and Kelch [6]. The SMPs of interest in this work are chemically cross-linked thermosets, for which the cross-linked regions maintain the permanent shape of the polymer. In these SMPs, the glass transition temperature serves as the transition temperature necessary for shape recovery.

At temperatures above the glass transition temperature (T_g), the polymer is in the rubber phase, and the stiffness is lower than when the temperatures are below T_g. Consequently, large scale deformations are possible as the polymers are able to move and stretch with ease. On the other hand, when $T < T_g$ and the polymer is in the glass phase, the large-scale motions are prevented due to the increased stiffness of the polymer. As a result, only smaller, local elastic motions are possible in the glass phase – resulting in smaller allowable elastic strains. Furthermore, a material which undergoes deformation in the rubber phase can be “frozen” by maintaining the deformation while cooling to the glass phase. Once in the glass phase, the polymers affected by the deformation process will be indefinitely frozen until subsequent heating.

The complete thermomechanical cycle allowing for the shape memory effect is outlined in the

following steps. In addition, Figure 1 presents the thermomechanical cycle in stress-strain-temperature space and relates it to the schematic, molecular representation of the shape memory effect.

1. Deform the SMP at $T > T_g$ (rubber phase) to the desired strain level. By loading in the rubber phase, large strains can be generated as molecular chains are stretched. The entropy of the system is reduced due to the imposed deformation.
2. Hold the applied strain constant, and cool to below T_g. The strain is stored as the stiff glass phase prevents the molecular chains from moving, and the new configuration is termed the temporary shape.
3. Unload the specimen at $T < T_g$ (glass phase) to a predetermined stress level (i.e. zero stress). The decrease in strain due to elastic unloading in the glass phase is negligible.
4. Hold the stress level constant, and heat the material to above T_g. The molecular chains are free to move, and return to their original, permanent shape – a state of higher entropy than the original shape.

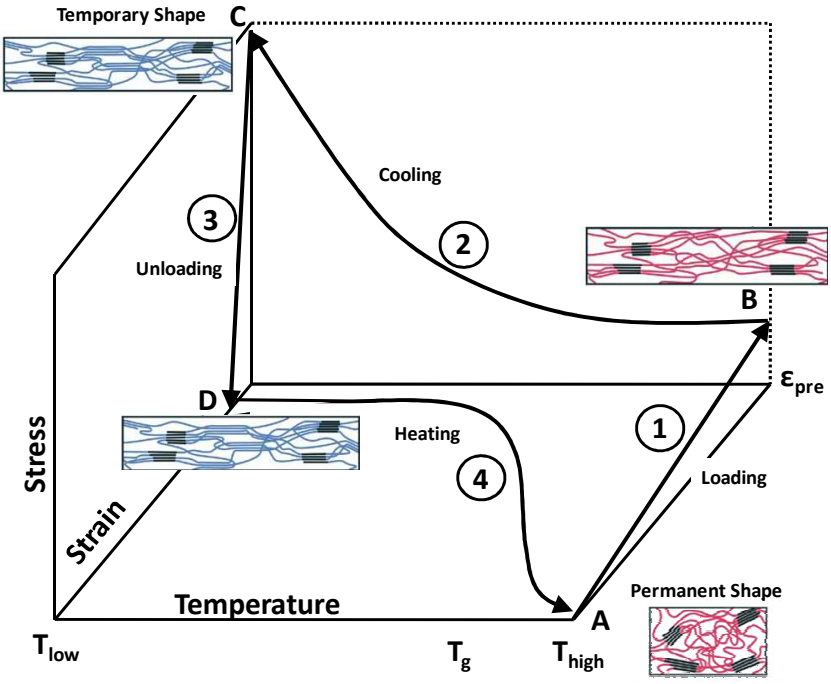

Figure 1 – Shape memory effect thermomechanical cycle and schematic molecular representation.

3. EXPERIMENTAL PROCEDURES

As noted in the previous section, the thermomechanical cycle for SMPs is detailed, and consequently requires a detailed experimental approach. This section presents the experimental setup and methods used to thermomechanically characterize the SMPs.

3-1. Experimental Setup

All of the thermomechanical experiments on the shape memory polymers were performed in the Materials Research Laboratory at NASA Langley Research Center. The tests were conducted on a vertical electromechanical, screw-driven MTS Alliance RT-1 test frame which utilized a MTS 1000

N load cell and a pair of MTS 2000 N pneumatic grips equipped with serrated grip faces. With the pneumatic grips, a grip pressure can be consistently selected as to neither yield the specimen in the grip region nor allow slipping of the material during loading. The grip pressure used for these tests was 80 kPa.

In addition, the thermomechanical characterization of SMPs requires a complex, multi-step temperature profile with a controlled temperature rate. Consequently, the experimental setup included a Thermcraft temperature chamber and controller with forced convection heating and liquid nitrogen cooling. The temperature range of the chamber was -73°C to 315°C. The temperature was measured by a thermocouple placed near the gage region of the specimen. Due to the large size of the pneumatic grips and the fact that the thermocouple reads the air surrounding the specimen, the stress upon cooling the material while holding the deformation constant continues to increase after the thermocouple indicates the system is at room temperature. As a result, a dwell time is necessary upon heating and cooling to allow the system to reach thermal equilibrium. Figure 2a depicts the entire experimental setup, and Figure 2b presents a view of the specimen inside the pneumatic grips.

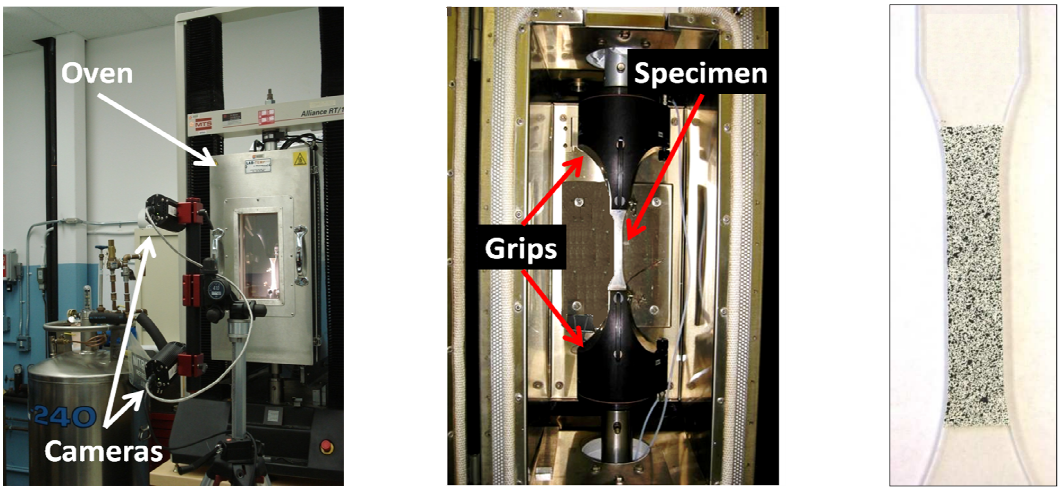

Figure 2 – (a) Complete experimental setup, (b) View inside temperature chamber, and (c) Specimen ready for use with VIC 3D system.

Due to the low elastic modulus of shape memory polymers at high temperatures, non-contact strain measurement techniques, such as optical or laser extensometers, are generally more desirable for thermomechanical characterization to ensure that no interference of specimen motion occurs. Furthermore, such techniques generally offer the capability of measuring larger deformations. For the experiments presented in this work, the strain was measured and recorded using the VIC 3D strain measurement technique. Developed by Correlated Solutions, Inc., the VIC 3D system provides the ability to calculate the displacement of a material point in the three principal directions as well as the full-field, two-dimensional strain measurements. The VIC 3D system begins by taking a picture of the reference configuration and a picture of the specimen at each specified time interval. At each interval, the system calculates the displacement of the material point in the current configuration from the reference configuration. Using these displacements, the VIC 3D system calculates the complete Lagrange strain tensor.

To prepare a specimen for use with this system, a high-contrast ``speckled" pattern is painted on the surface of the gauge area, as seen in Figure 2c. Because the SMP specimens were transparent, a white base coat was first applied to the specimens. The random, black speckled pattern was subsequently applied to achieve the necessary contrast.

3-2. Material Preparation

The material used for testing is the commercially available Veriflex™ from Cornerstone Research Group, Inc.(CRG) in Dayton, Ohio. Veriflex™ is a thermoset, polystyrene-based shape memory polymer. With the current experimental focus strictly on tension tests, the specimens were prepared to a size adapted from the ASTM D638 Standard Test Method for the Tensile Properties of Plastics [18]. The resulting samples were in a dogbone shape with a 57.0 mm gauge length and a 12.7 mm x 3.2 mm cross-sectional area in the gauge region. The total length of the specimens was 114.0 mm. A water jet cutting procedure, performed at NASA Langley Research Center, was used to cut the experimental specimens from the bulk material. Although the water jet cutting procedure increases the consistency of the specimen dimensions, the procedure can create small stress waves at the end point on each specimen. As a result, it is important to have the start/finish point at the far ends of the specimen such that any material damage does not affect the material response of the gage area.

3-3. Thermomechanical Parameters

The experimental characterization for the shape memory polymers followed the thermomechanical cycle outlined in Section 2.1. The specimen was placed in the temperature chamber at room temperature. After placement of the specimen, the temperature chamber was heated from room temperature to approximately 30 degrees above the glass transition temperature T_g. As noted in the literature and verified by DSC experiments, the transition from the glass phase to the rubber phase occurs over a range of temperatures, rather than an instantaneous transition at T_g [6,9]. Consequently, the Tg is calculated from the DSC results as approximately 60°C, with complete transformation occurring at 85°C. The reverse transformation (to the glass phase) is complete at 40°C. As a result, the specimen is heated to 90°C at 2°C/min to ensure the specimen is completely in the rubber phase. After reaching thermal equilibrium, the specimen is loaded at a rate of 0.025 (mm/mm)/min to a predetermined extension (values ranging from 10 to 100%). After reaching the desired strain value, the deformation is held constant, and the specimen is cooled to room temperature (25°C) at 2°C/min to ensure complete transformation to the glass phase. The constrained cooling induces a stress increase, which is consequently unloaded after cooling is complete. Finally, zero load is maintained on the specimen, and the temperature is again raised to 90°C at 2°C/min to induce strain recovery.

4. RESULTS

This section will present representative thermomechanical results for experiments with an applied extension of 10 to 100%. In addition, the strain calculated from the material displacement will be compared with the strain calculated at the material points at the ends of the gage area, as calculated via the VIC 3D system.

4-1. Strain Measurements

Due to the fact that the VIC 3D system is not capable of real-time strain readings, the loading segment of the thermomechanical load path is controlled by the crosshead displacement. As a result, the software loads the specimen to 10, 25, 50, and 100% extension as calculated by the initial grip separation and crosshead displacement. Using the VIC system to calculate the extension of the specimen, the SMP specimens underwent extensions of approximately 9, 26, 53, and 107%.

Furthermore, the VIC system calculates the Lagrange strain for each material point, as

measured at individual pixels. In this study, the axial Lagrange strain was calculated for a material point on each end of the gage area. These two strains were compared to the average axial Lagrange strain for the entire gage area. The values for the two end points as well as the average value of the specimen are shown in Figure 3 for extensions of 25 and 100%. The Lagrange strain for the specimen is approximately 30 and 160% in for the 25 and 100% extension experiments, respectively.

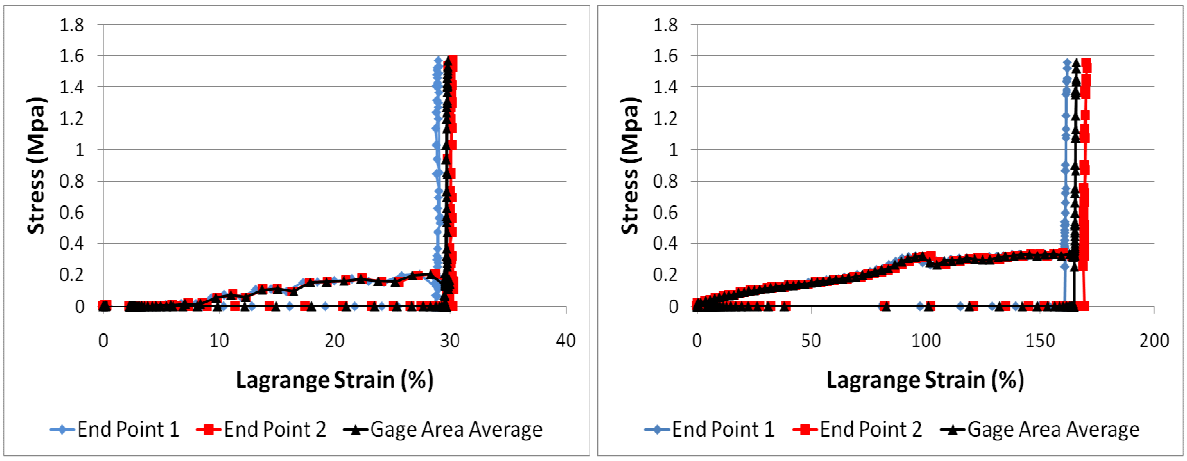

Figure 3 – Comparison of Lagrange strains calculated at end points of gage area and the average value for the entire gage area for (a) 25% extension, (b) 100% extension.

4-2. Tensile Strain Recovery Experiments

Shape memory polymer specimens were stretched to extensions of 10, 25, 50, and 100%. A representative result for each extension value is shown in Figure 4. These experiments are tested according to the thermomechanical parameters outlined in Section 3.3. The specimens begin in a stress-free and strain-free initial state at room temperature (25°C) and are loaded under strain control to the predetermined extension level, at which point the deformation is held constant while the temperature is cooled from 90°C to 25°C. The constrained cooling induces a stress in the material, which is subsequently unloaded upon completion of the cooling procedure. After unloading, the zero load is maintained, and the temperature is again raised to 90°C to allow for recovery of the applied strain. In the 10, 25, and 50% extension experiments, the specimen has recovered all of the extension applied to the material while $T > T_g$. In the 100% extension experiment, the value of the extension at the end of the test is higher than that of the reference configuration (at the end of the initial heating to 90°C). This difference in recoverable extension may be attributed to the inflection in the stress-strain portion of Figure 3b, which may indicate the onset of yielding in the material.

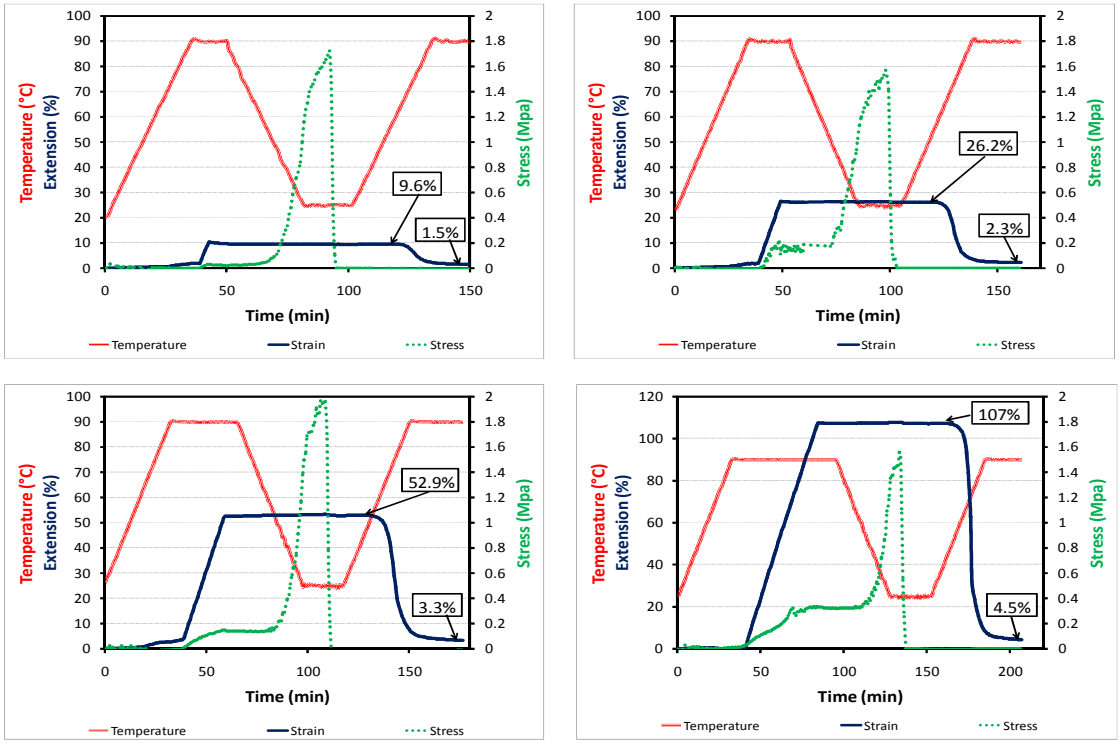

Figure 4 – Stress-strain-temperature results for tensile tests with extensions of 10% (top left), 25% (top right), 50% (bottom left), and 100% (bottom right).

4-2-1. Stress-Strain Relationship

The stress-strain relationship for the 10, 50, and 100% extension experiments is presented in Figure 5a. In addition, Figure 5b focuses on the loading segment of the thermomechanical load path in the experiments. From the figures, it is clear that the stress-strain relationship follows the same trend during initial loading. At greater extensions, the stress-strain behavior deviates from a linear relationship and begins to flatten. A peak is observed during the 100% extension experiment, indicating the beginning of yielding in the specimen.

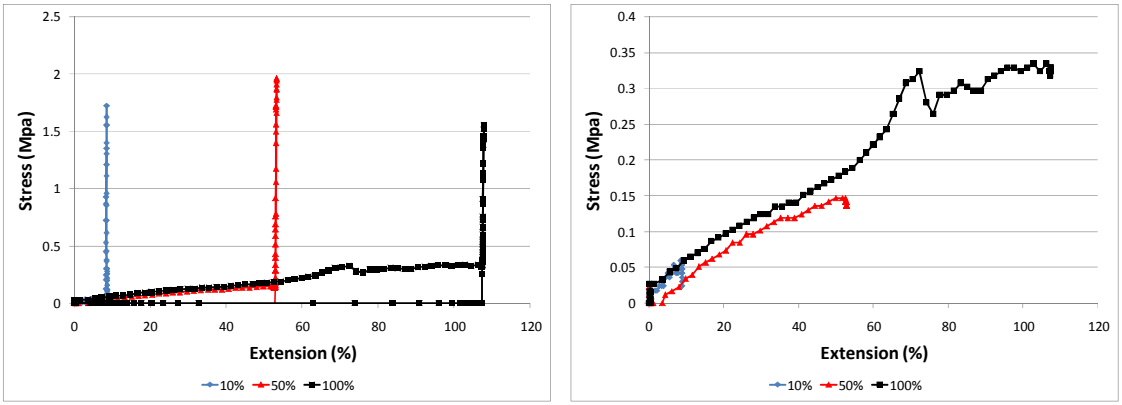

Figure 5 – Stress-strain results for tensile tests with extensions of 10%, 50%, and 100%, where (a) is the entire experiment, and (b) is the loading portion of the test.

4-2-2. Strain-Time Relationship

The strain-time relationship for the 10, 50, and 100% extension experiments is presented in Figure 6. In this figure, the recovery time for each experiment is offset for purposes of comparison. From the figure, it is clear that time rate of change of the extension during recovery is greater with increasing values of extension, with the 10% extension experiment displaying a gradual shape recovery and the 100% extension experiment displaying a very sharp shape recovery.

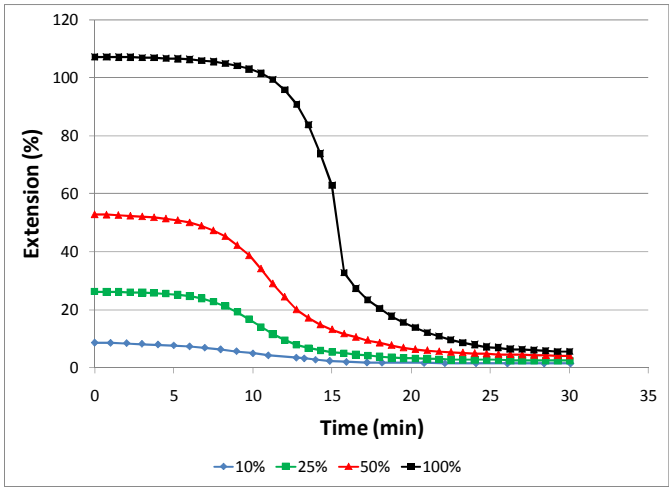

Figure 6 – Strain-time results for tensile experiments of 10%, 25, 50%, and 100% extension.

5. CONCLUSIONS

A series of thermomechanical experiments were performed on shape memory polymer specimens such that the applied extensions were 10, 25, 50, and 100%. The thermomechanical cycle necessary for the shape memory effect was presented and related to the state of the molecular chains for the type of SMP chosen for the particular experiments. In addition, the experimental setup was constructed in such a way as to allow for large deformations of SMPs in a way such that the temperature and load profiles could be easily adjusted for arbitrary thermomechanical load paths. The axial Lagrange strain of the two endpoints of the gage area was compared to the average Lagrange strain of the entire gage area, for which the average value fell between the values of the two endpoints. In addition, the stress-strain behavior was analyzed for the tensile tests, in which the stress-strain relationship deviated from linear at values of extension greater than 10%. Finally, analysis of the results demonstrates the increased rate of shape recovery with increasing extension values.

ACKNOWLEDGEMENTS

The authors would foremost like to acknowledge Cornerstone Research Group for their discussions on the material properties and behavior of the Verifex SMP. In addition, the authors would like to acknowledge Karen Whitley of NASA Langley Research Center for her guidance and assistance on performing the experimental work reported in this paper. Funding for the work of B. Volk is provided by the National Science Foundation Integrated Graduate Education and Research Traineeship (IGERT) Fellowship administered by Texas A&M University.

REFERENCES

1. K. Otsuka and C. Wayman, Shape Memory Materials, Cambridge University Press, New York, NY, 1999.
2. A. Srinivasan and D. McFarland, Smart Structures: Analysis and Design, Cambridge University Press, Cambridge, 2001.
3. D. J. Hartl and D. C. Lagoudas, “Aerospace applications of shape memory alloys," Journal of Aerospace Engineering 221, pp. 535-552, 2007.
4. K. Gall, M. Mikulas, N. Munshi, F. Beavers, and M. Tupper, “Carbon fiber reinforced shape memory polymer composites," Journal of Intelligent Material Systems and Structures 11, pp. 877-886, 2000.
5. Y. Liu, K. Gall, M. Dunn, A. Greenberg, and J. Diani, “Thermomechanics of shape memory polymers: Uniaxial experiments and constitutive modeling," International Journal of Plasticity 22, pp. 279- 313, 2006.
6. Lendlein and S. Kelch, “Shape-memory polymers," Angew. Chem. Int. Ed. 41, pp. 2034-2057, 2002.
7. H. Tobushi, T. Hashimoto, S. Hayashi, and E. Yamada, “Thermomechanical constitutive modeling in shape memory polymer of polyurethane series," Journal of Intelligent Material Systems and Structures 8, pp. 711-718, 1997.
8. H. Tobushi, T. Hashimoto, N. Ito, S. Hayashi, and E. Yamada, “Shape fixity and shape recovery in a thin film of shape memory polymer of polyurethane series," Journal of Intelligent Material Systems and Structures 9, pp. 127-136, 1998.
9. C. Liu, H. Qin, and P. T. Mather, “Review of progress in shape-memory polymers," Journal of Materials Chemistry 17, pp. 1543-1558, 2007.
10. V. A. Beloshenko, V. N. Varyukhin, and Y. V. Voznyak, “The shape memory effect in polymers," Russian Chemical Reviews 74, pp. 265-283, 2005.
11. D. Ratna and J. Karger-Kocsis, “Recent advances in shape memory polymers and composites: A review," Journal of Materials Science 43, pp. 254-269, 2008.
12. K. Gall, M. Dunn, Y. Liu, D. Finch, M. Lake, and N. Munshi, “Shape memory polymer nanocomposites," Acta Materialia 50, pp. 5115-5126, 2002.
13. T. Ohki, Q. Ni, N. Ohsako, and M. Iwamoto, “Mechanical and shape memory behavior of composites with shape memory polymer," Composites: Part A 35, pp. 1065-1073, 2004.
14. Z. G. Wei, R. Sandstrom, and S. Miyazaki, “Shape-memory materials and hybrid composites, part I: Shape-memory materials," Journal of Materials Science 33, pp. 3743-3762, 1998.
15. Z. G. Wei, R. Sandstrom, and S. Miyazaki, “Shape memory materials and hybrid composites, part II: Shape-memory hybrid composites," Journal of Materials Science 33, pp. 3763-3783, 1998.
16. H. Tobushi, K. Okumura, S. Hayashi, and N. Ito, “Thermomechanical constitutive model of shape memory polymer," Mechanics of Materials 33, pp. 545-554, 2001.
17. B. Atli, F. Gandhi, and G. Karst, “Thermomechanical characterization of shape memory polymers," in Electroactive Polymer Actuators and Devices, Proceedings of SPIE Vol. 6524, Y. Bar-Cohen, ed., pp. 65241S1-10, SPIE, 2007.
18. ASTM International, “D638-03: Standard test method for tensile properties of plastics," ASTM